

Improvement of Photoluminescence of Graphene Quantum Dots with a Biocompatible Photochemical Reduction Pathway and Its Bioimaging Application

Hanjun Sun,^{†,‡} Li Wu,^{†,‡} Nan Gao,[†] Jinsong Ren,[†] and Xiaogang Qu^{*,†}

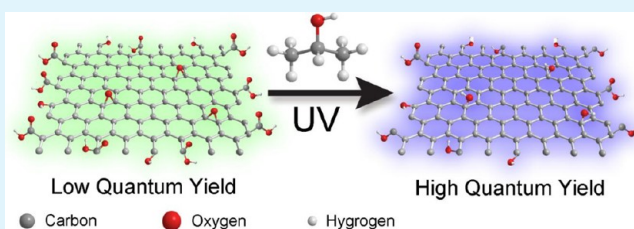
[†]Laboratory of Chemical Biology, Division of Biological Inorganic Chemistry, State Key Laboratory of Rare Earth Resource Utilization, Changchun Institute of Applied Chemistry, Chinese Academy of Sciences, Changchun, Jilin 130022, P. R. China

[‡]Graduate School of the Chinese Academy of Sciences, Beijing, 100039, P. R. China

S Supporting Information

ABSTRACT: As a rising star in the family of fluorescent material, graphene quantum dots (GQDs) have attracted great attention because of their excellent properties such as high photostability against photobleaching and blinking, biocompatibility, and low toxicity. Herein, blue luminescent GQDs were prepared by photo-reducing GQDs with isopropanol. After photochemical reduction, the increasing of sp^2 domains and the formed hydroxyl in pGQDs can enhance the photoluminescence of GQDs. The quantum yield of the photo-reduced GQDs (pGQDs) was increased 3.7 fold. Because of its less negative surface charges and lower cytotoxicity than chemical reduced GQDs (cGQDs), the pGQDs were more easily uptaken by cells. This work may provide a simple and green pathway to enhance the QY of GQDs with satisfactory biocompatibility as fluorescent nanoprobes.

KEYWORDS: graphene quantum dots, photochemical reduction, photoluminescence, cytotoxicity, cell imaging



1. INTRODUCTION

Graphene quantum dots (GQDs), as their cousin, carbon dots (CDs), have attracted great attention since they were first reported in 2008.¹ As a kind of fluorescent material, GQDs have excellent properties such as high photostability against photobleaching and blinking, biocompatibility, and low toxicity like CDs. However, like CDs, the quantum yield (QY) of GQDs is usually very low. Therefore, the preparation of GQDs with high QY is demanding and important.^{2,3} To this end, many methods for modulating the fluorescence emission spectra of GQDs and improving its QY have been reported.^{2,3}

Chemical reduction and surface passivation are the most common pathways to improve the QY of GQDs. Zhu et al. used NaBH_4 as reducing agent to convert greenish-yellow luminescent GQDs (gGQDs) synthesized by microwave-assisted method, to bright blue luminescent GQDs with higher QY.⁴ Shen et al. prepared the GQDs passivated by PEG, and found the QY of as-prepared GQDs-PEG with 360 nm emission was up to 28%, which was two times higher than the pristine GQDs.⁵ However, chemical reduction and surface passivation often take a long reaction time and introduce toxic reagents.^{4–7} Thus, it is very important to find a fast and eco-friendly strategy to enhance the QY of GQDs with satisfactory biocompatibility.

Compared with conventional chemical reduction, the photochemical reduction method is “green” and easy to control via irradiation.⁸ And it is widely used in preparing metal nanoparticles, and reduced graphene sheets.^{9–12} To the best of

our knowledge, there has been no report by using photochemical reduction method to enhance the photoluminescence (PL) of GQDs.

In this paper, we use alcohols as the reducing agent assisted with UV irradiation to prepare bright blue luminescent GQDs with high QY through photo-reducing pathway. Compared to the traditional chemical reduction (NaBH_4 or $\text{N}_2\text{H}_4\cdot\text{H}_2\text{O}$ used as reducing agent), the photochemical reduction only takes several minutes, which is much faster than chemical reduction (usually needs several hours).^{4–7} Furthermore, the prepared GQDs would be more biocompatible because of not using toxic reagents.^{13,14} Therefore, photochemical reduction can be used to eco-friendly improve QY of GQDs, and the as-prepared GQDs has lower toxicity and can be used as a promising biomaterial in biology and medical imaging.

2. EXPERIMENTAL SECTION

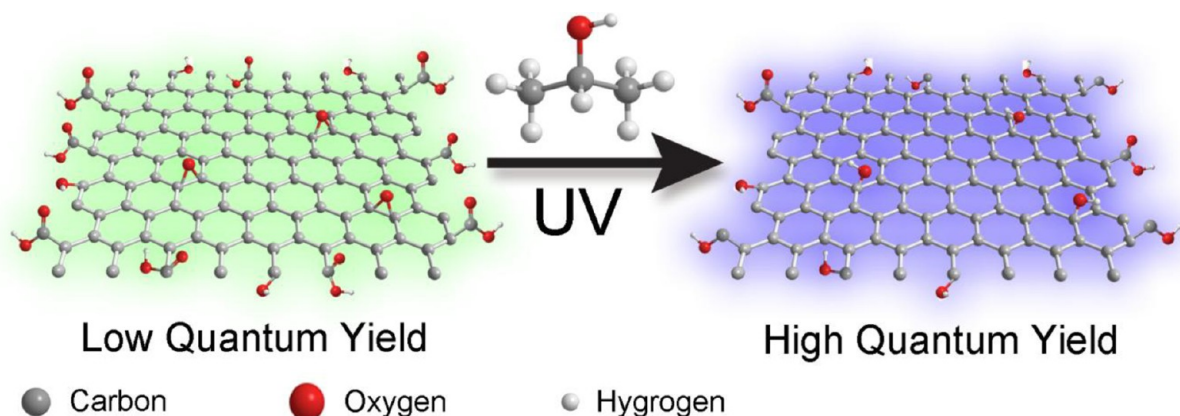
2.1. Materials. Graphite was purchased from Sinopharm Chemical Reagent Co. Ltd. (Shanghai, China). Sulfuric acid, nitrate and isopropanol were provided by Beijing Chemicals Inc. (Beijing, China). Sodium borohydride (NaBH_4) were purchased from Alfa Aesar. Fluorescein was purchased from Sigma-Aldrich. Quinine sulfate was purchased from Aladdin Chemistry Co. Ltd. (Shanghai, China). Dialysis bags (molecular weight cut off = 1000 and 3500) were ordered from Shanghai Sangon biotechnology Development Co., Ltd.

Received: December 12, 2012

Accepted: January 22, 2013

Published: January 22, 2013

Scheme 1. Schematic Representation of the Preparation Route for pGQDs



Ultra-pure water was prepared using a Milli-Q-Plus system water (18.2 M Ω cm) and used in all experiments. All reagents were used as received without any further purification.

2.2. Synthesis of gGQDs. Graphene oxide (GO) was synthesized from graphite by a modified Hummers method.¹⁵ GO solution (30 mL, 0.5 mg/mL) was first mixed carefully with concentrated HNO₃ (8 mL) and H₂SO₄ (2 mL). Then the mixture was heated and refluxed under microwave irradiation for 9 h in a WBFY-201 Microwave Oven equipped with atmospheric reflux device (Gongyi Instrument Equipments Co. Ltd., China) operating at a power of 650 W. The product contained brown transparent suspension and black precipitates. After cooling to room temperature, the mixture was under mild ultrasonication for few minutes, and the pH was tuned to 8 with Na₂CO₃ in an ice-bath. The suspension was filtered through a 0.22 μ m microporous membrane to remove the large tracts of GO and a deep yellow solution (yield ca. 30%) was separated. The mixture solution was further dialyzed in a dialysis bag (retained molecular weight: 1000 Da) and greenish yellow fluorescent GQDs were obtained.⁴

2.3. Synthesis of cGQDs. The above obtained deep yellow filter solution was reduced with NaBH₄ (1 g) under vigorous stirring at room temperature for 2 h. The solution color faded to yellow. Then HNO₃ solution was added dropwise to terminate the reaction and tuned the pH to 8. The suspension was filtered through a 0.22 μ m microporous membrane and further dialyzed in a dialysis bag (retained molecular weight: 1000 Da) to obtain brightly blue luminescent GQDs.⁴

2.4. Synthesis of Carbon Dots (CDs). CDs were prepared as described previously.¹⁶ Briefly, candle soot was collected by putting a piece of glass plate on top of burning unscented candles. 100 mg of candle soot was mixed with 20 mL of 5 mol/L nitric acid in a 50 mL three-necked flask. The mixture was then refluxed for 12 h with magnetic stirring. After being cooled to room temperature, the black solution was centrifuged at 12 000 rpm for 30 min. The fluorescent CDs supernatant was collected, neutralized by Na₂CO₃, and extensively dialyzed against Millipore 18.2 M Ω cm water through a dialysis membrane (retained molecular weight: 1000 Da).

2.5. Synthesis of pGQDs and pCDs. Photochemical reactions were carried out in 1 cm quartz cuvettes. The cuvette filled with mixture solution of 3 mL pGQDs or pCDs solution and 30 μ L isopropanol was placed horizontally for UV irradiation under a high-pressure mercury lamp (500 W, 50W/cm², GY-500, Beijing Tianmai Henghui Lighting & Electrical Appliance Co., Ltd., Beijing, China) at a distance of 30 cm for 30 min and further dialyzed in a dialysis bag (retained molecular weight: 1000 Da) to obtain brightly blue luminescent pGQDs and pCDs.

2.6. Apparatus and Characterization. UV absorbance measurements were carried out on a JASCO V-550 UV-vis spectrophotometer, equipped with a Peltier temperature control accessory. Fluorescence spectra were measured on a JASCO FP-6500 spectrofluorometer equipped with a temperature-controlled water

bath. Upconversion fluorescence spectra were measured on a Hitachi F-7000 spectrofluorometer equipped with a temperature-controlled water bath. All spectra were recorded in a 1.0 cm path length cell. FT-IR characterization was carried out on a BRUKER Vertex 70 FT-IR spectrometer. The samples were thoroughly ground with exhaustively dried KBr. AFM measurements were performed using Nanoscope V multimode atomic force microscope (Veeco Instruments, USA). TEM images were recorded using a FEI TECNAI G2 20 high-resolution transmission electron microscope operating at 200 kV. Cellular Imaging was visualized using an Olympus BX-51 optical system microscope (Tokyo, Japan). Pictures were taken with an Olympus digital camera.

2.7. Cell Culture. Human lung adenocarcinoma A549 cells were cultured in 25 cm² flasks in Dulbecco's Modified Eagle's Medium DMEM (Gibco) containing 10% (v/v) fetal bovine serum (Gibco) at 37 $^{\circ}$ C in an atmosphere of 5% (v/v) CO₂ in air. The media were changed every 48 h, and the cells were passaged by trypsinization before confluence.¹⁷

2.8. MTT Assay. The toxicity of pGQDs and cGQDs to cells was measured by MTT assay.^{17,18} Briefly, A549 cells were plated at a density of 1×10^4 cells per well in 100 μ L of RPMI medium in 96-well plates and grown for 48 h. The cells were then exposed to a series of concentrations of pGQDs and cGQDs for 48 h, and the viability of the cells was measured using the methylthiazolotetrazolium method. Controls were cultivated under the same conditions without the addition of the GQDs. Then, 5 μ L of MTT (5 mg/mL) was added into the wells and further incubated for an additional 4 h. Subsequently, the supernatant was discarded, followed by the additional of 100 μ L DMSO into each well and incubation in the shaker incubator with gentle shakes. Then the optical density (OD) was read at a wavelength of 570 nm. Relative inhibition of cell growth was expressed as follows: % = $(1 - [\text{OD}]_{\text{test}} / [\text{OD}]_{\text{control}}) \times 100$.

2.9. Cellular Imaging. A549 cells were seeded in a 24-well plate and cultured for 24 h. The cell medium was removed, and then cells were incubated with 0.5 mL of fresh cell medium containing 50 μ g of cGQDs or pGQDs for 24 h. After that, cell imaging was then carried out after washing cells with PBS for three times.^{17,18}

2.10. Quantum Yield (QY) Measurements. Quinine sulfate in water (QY = 0.577) was chosen as a standard with pGQDs and cGQDs. And Fluorescein in water (QY = 0.95) was chosen as a standard with gGQDs. The quantum yields of gGQDs, pGQDs and cGQDs in water were calculated according to the formula: $\Phi = \Phi_s (I/I_s) (A/A_s) (n_s/n)^2$.^{4,16}

Where Φ is the quantum yield, I is the measured integrated emission intensity, n is the refractive index of the solvent (1.33 for water), and A is the optical density. The subscript "s" refers to the reference standard with known quantum yield. To minimize reabsorption effects, absorbencies in the 10 mm fluorescence cuvette were kept under 0.1 at the excitation wavelength (gGQDs at 480 nm, pGQDs and cGQDs at 340 nm).

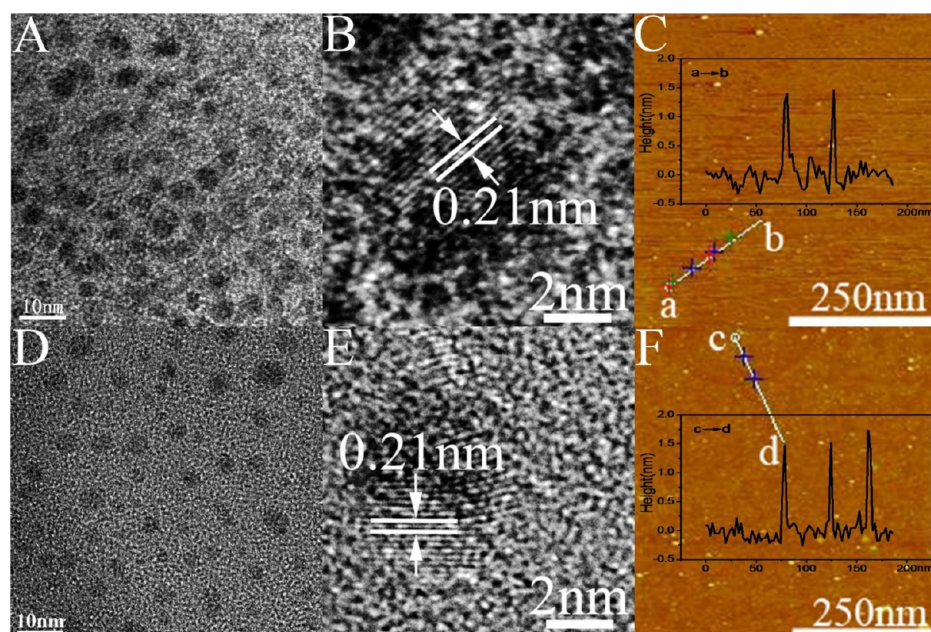


Figure 1. TEM images of (A) gQDs and (D) pQDs. (B, E) Representative images of individual gQDs and pQDs. The AFM images of (C) gQDs and (F) pQDs, respectively. Insets of C and F are corresponding height profiles of gQDs and pQDs, respectively.

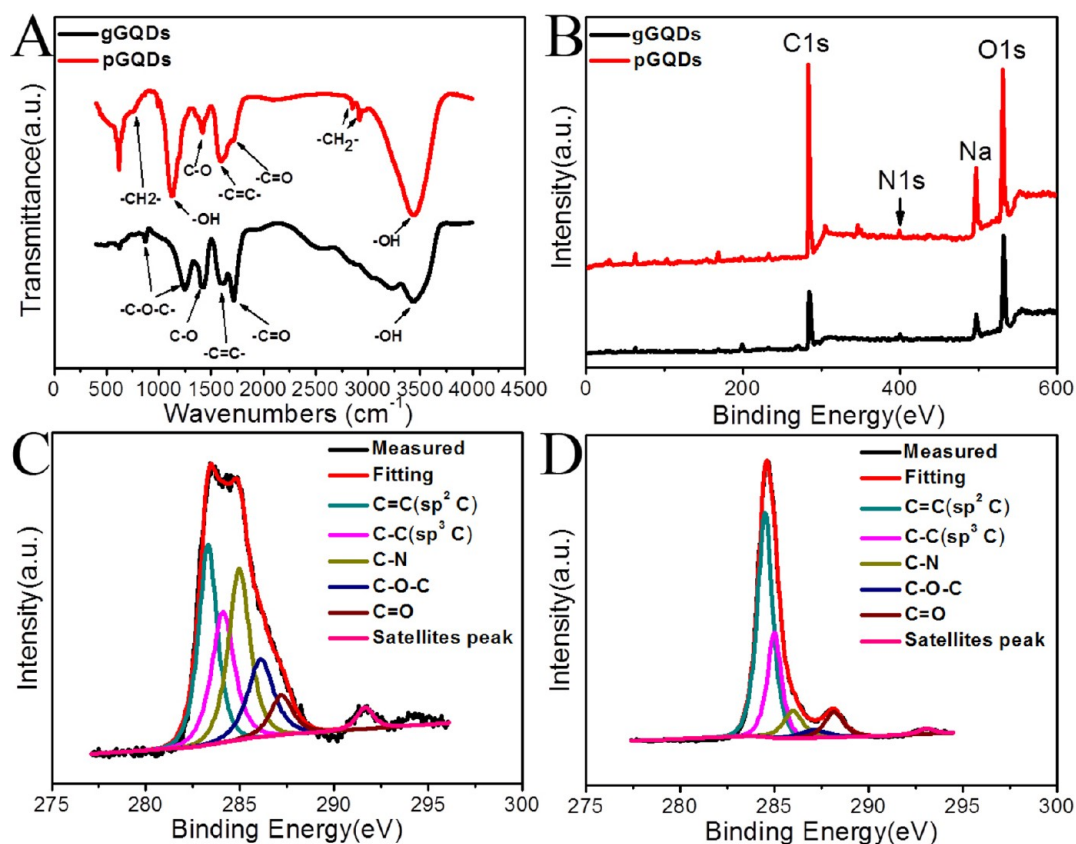


Figure 2. (A) FT-IR spectra of gQDs, and pQDs. (B) XPS analysis surveys of gQDs and pQDs. The XPS C1s analysis of (C) gQDs and (D) pQDs.

3. RESULTS AND DISCUSSION

3.1. Structural Characterization. As shown in Scheme 1, gQDs which emit green luminescence were synthesized as previously reported,¹⁴ and then they were photoreduced by isopropanol with UV lamp (365 nm, 500 W, 50W/cm²) at a

distance of 30 cm for 30 min. The obtained photochemically reduced GQDs (pGQDs) showed an increase in the blue-shifted luminescence. Using other alcohols, such as methanol and ethanol, the prepared pGQDs showed similar increase in the blue-shifted luminescence (data not shown). The obtained pGQDs were stable for at least six months under ambient

Table 1. XPS Analysis and Zeta Potentials of gGQDs, pGQDs and cGQDs

sample	C=C and C-C (%)	oxygenated C and nitrous C (%)	carbon contents (%)	oxygen contents (%)	nitrogen contents (%)	zeta potential (mV)
gGQDs	52.15	47.85	52.74	43.90	3.36	-21
pGQDs	80.12	19.88	71.66	25.08	3.26	-5
cGQDs	70.24	29.76	63.51	33.21	3.28	-14

temperature conditions. The typical transmission electron microscope (TEM) images showed that both gGQDs and pGQDs were well dispersed (Figure 1A, D). For gGQDs and pGQDs, their size distribution (3–9 nm) and the average size (5.6 nm) was similar (see Figure S1A, B in the Supporting Information), which indicated that photochemical reduction did not change the size of GQDs. The typical atomic force microscopy (AFM) images showed their height distributions of gGQDs and pGQDs were 0.5–2.5 nm, and the average heights of gGQDs and pGQDs were 1.5 and 1.6 nm (see Figure S1C, D in the Supporting Information), respectively, indicating that both gGQDs and pGQDs meet the definition of the GQDs.² Furthermore, high-resolution TEM (HRTEM) images showed both of the two kinds of GQDs had crystallinity with lattice of 0.21 nm, which was consistent with the (102) diffraction planes of sp^2 graphitic carbon, and indicated that the two kinds of GQDs kept the similar crystallinity with graphene.¹⁹ Figure 1 showed the dimension and height of pGQDs and gGQDs had no obvious change, indicating that the luminescence blue-shift of pGQDs could be attributed to their chemical structural change after reduction rather than their dimension variation.

Fourier transform infrared (FT-IR) spectroscopy and X-Ray photoelectron spectroscopy (XPS) were used to study the surface groups of GQDs. As shown in Figure 2A, stretching vibrations of C–OH at 3430 cm^{-1} , C=C at 1595 cm^{-1} and C=O at 1715 cm^{-1} were observed for both gGQDs and pGQDs. However, the vibrational absorption bands of C–O–C at 1250 cm^{-1} and 876 cm^{-1} were observed only for gGQDs. After photochemical reduction, the vibrational absorption band of C=O was weakened, whereas vibrations of –OH at 1125 cm^{-1} and stretching vibrations of C–H at 2920 and 2850 cm^{-1} were observed in pGQDs, indicating that the C=O and C–O–C groups were photoreduced to C–OH and the edge of pGQDs existed alkyl.^{19,20} Furthermore, the XPS of the gGQDs and pGQDs showed three types of carbons: graphitic carbon (C=C and C–C), oxygenated carbon (C=O and C–O–C), and nitrogenated carbon. The nitrogen originated from HNO_3 oxidation which induced doping of nitrogen into GQDs through a small extent of nitration.⁴ The percentages of oxygen-bonded carbon in pGQDs decreased progressively in comparison with gGQDs (Table 1), showing that the groups of C–O–C and C=O in the GQDs were reduced during UV irradiation, consistent with the results of FT-IR. Further analyses indicated that the ratio of sp^2 carbon (C=C) and sp^3 carbon (C–C) was 1.3:1 and 2.3:1 in gGQDs and pGQDs, respectively, which illustrated sp^2 carbon increased upon photochemical reduction.^{7,21} The contents of carbon, oxygen, and nitrogen in gGQDs were 52.74, 43.90, and 3.36%, whereas in pGQDs, the values were 71.66, 25.08, and 3.26%, respectively. Both the decreased percentages of oxygen-bonded carbon and the increased contents of carbon indicated the reduction occurred during the UV irradiation.⁴ The zeta potential of gGQDs and pGQDs were –21 and –5 mV (pH 7.0), respectively. This indicated that reduction decreased the surface charges of gGQDs (Table 1).⁴

3.2. Optical Characterization. The optical properties of gGQDs and pGQDs were studied by using UV–vis absorption and photoluminescence spectroscopy. In the UV–vis absorption spectra (see Figure S2 in the Supporting Information), the maximum peak of both gGQDs and pGQDs were located at 270 nm. A new absorption band at 340 nm appeared for pGQDs, whereas the absorption peak at 460 nm was not observed for gGQDs, which was caused by the surface change of GQDs.⁶ As shown in Figure 3 and Figure S3 in the

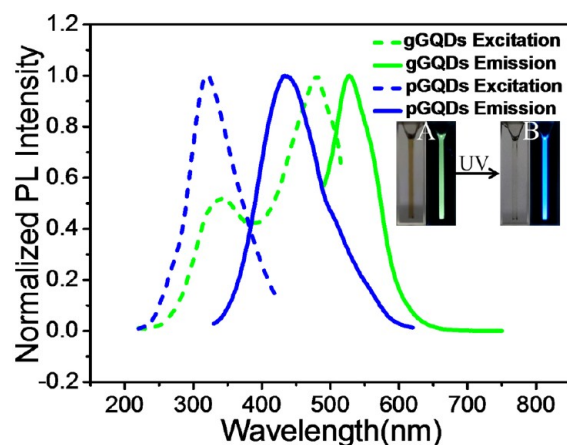
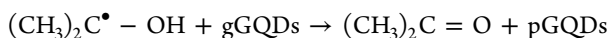
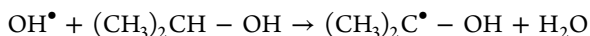
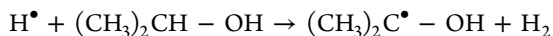
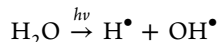


Figure 3. Normalized photoluminescence spectra of the gGQDs (the excitation wavelength of the emission spectrum was 480 nm and the emission wavelength of the excitation spectrum was 540 nm) and the pGQDs (the excitation wavelength of the emission spectrum was 320 nm and the emission wavelength of the excitation spectrum was 440 nm). Insert: photograph of the (A) gGQD and (B) pGQDs aqueous solution taken under visible light and 365 nm UV light, from left to right, respectively.

Supporting Information, the gGQDs exhibited maximum excitation and emission wavelengths near 480 and 530 nm, respectively. However, when excited at 320 nm, the pGQDs showed bright blue photoluminescence and the emission was located at 440 nm (Figure 3). A blue-shifted upconversion luminescence of pGQDs was also observed (see Figure S4 in the Supporting Information). The average QYs of the pGQDs and gGQDs were 8.8% and 2.4%, respectively, showing that QY of the pGQDs was increased 3.7 fold, whereas the average QY of chemically reduced GQDs (cGQDs) was 8.5%, which indicated that both chemical reduction and photochemical reduction could improve the QYs of GQDs effectively (see Table S1 in the Supporting Information). According to the results of XPS and FT-IR, sp^2 domains increased upon reduction, and the formed hydroxyl in pGQDs might enhance the luminescence of GQDs.^{6,7,21} For demonstrating the generality of this photochemical reduction method, photo-reduction of the CDs prepared by refluxing candle soot in nitric acid was also carried out.¹⁶ After UV irradiation, the CDs also showed luminescence enhancement and blue-shifted from 520 to 450 nm (see Figure S5 in the Supporting Information).

3.3. Mechanism of Photochemical Reducing Graphene Quantum Dots. The mechanism was speculated as follows.⁹ When irradiated by UV light, the direct photolysis of H₂O generates H[•] and OH[•], then the isopropanol on the oxidation by H[•]/OH[•] yields (CH₃)₂C[•]-OH, which has strong reducing property as H atoms. (CH₃)₂C[•]-OH can reduce the oxidative groups on the gGQDs.⁹



The gGQDs consists of numerous disorder induced defect states within the $\pi-\pi^*$ gap and exhibits a luminescence spectrum centered at longer wavelengths. After the photochemical reduction, the number of disorder-induced states decreases, and an increased number of clusterlike states from the newly formed small and isolated sp² domains are formed. The electron-hole recombination among these sp² clusterlike states exhibits blue fluorescence at shorter wavelengths. The tunable luminescence spectra of GQDs during photochemical reduction are attributed to the variation of the relative intensity ratios of fluorescence emission from two different types of electronically excited states, changing the heterogeneous electronic structures of gGQDs and pGQDs with variable sp² and sp³ hybridizations through photochemical reduction.^{7,21} Furthermore, during the photochemical reduction, a great amount of electron-donating hydroxyl groups formats, can further enhance the luminescence of GQDs.⁶

3.4. Cellular Toxicity. To evaluate the cytotoxicity of the pGQDs and cGQDs, we carried out their effects on A549 cell line by using MTT method. As shown in Figure 4, in the

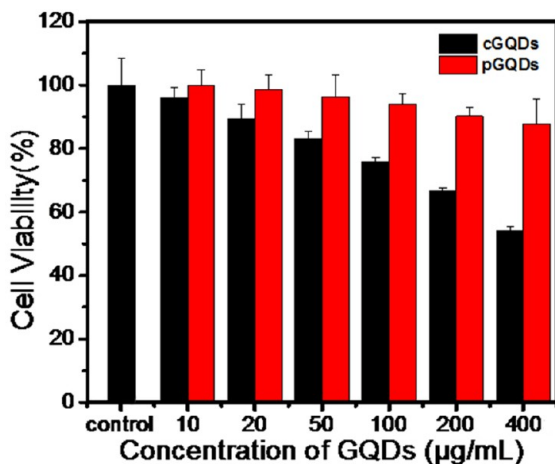


Figure 4. Cytotoxicity studies of the pGQDs and cGQDs (48 h post treatment) on A549 cells evaluated by the MTT method.

concentration range from 0 to 400 $\mu\text{g mL}^{-1}$ of GODs, parallel experiments showed that the cell survival rate in the presence of cGQDs was lower than that of pGQDs at any concentration. It should be pointed out that the concentration of the pGQDs we used here was much higher than those required for potential applications, such as optical imaging of living cells, and the exposure time was also much longer.^{17,18} The lower cytotoxicity

of pGQDs might be caused by using low toxic reagent during the photoreduction.

3.5. Cellular Imaging. Like CDs, GQDs can be used for biomedical imaging because of their stable PL, low cytotoxicity and excellent biocompatibility.^{2,3,19} Herein, we used cGQDs and pGQDs as fluorescent probes for imaging A549 cells. A549 cells were cultured in an appropriate culture medium containing the GQDs, and fluorescence microscope images were taken with an excitation wavelength of 380 nm. After incubation of 24 h, the cells displayed enhanced fluorescence around their nucleus (Figure 5), which indicated that both

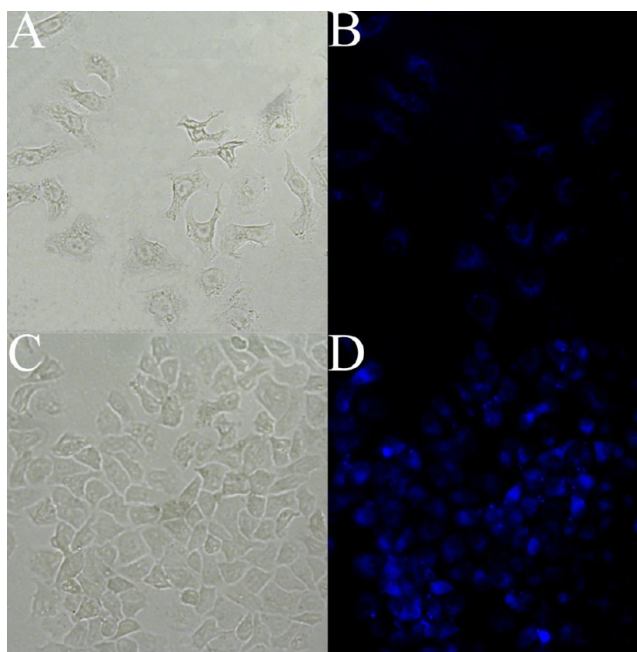


Figure 5. Cellular imaging of cGQDs: (A, B) are washed cells imaged under bright field, 380 nm, respectively; Cellular imaging of pGQDs: (C, D) are washed cells in bright field, 380 nm, respectively.

cGQDs and pGQDs were able to label the cell membrane and the cytoplasm.^{19,22,23} However, the stronger PL of pGQDs than cGQDs in A549 cells might indicate that pGQDs could be more easily uptaken by A549 cells due to less negative charges on pGQDs surfaces than that on cGQDs surfaces (Table 1),^{22,24} which might be derived from the less carboxyl on the surface of pGQDs (Figure 2, Figure S7 in the Supporting Information). The less negative charges on pGQDs promise them adhere to the negatively charged cell membrane more easily than cGQDs, thus achieving the effective uptaken by A549 cells.²⁴ Moreover, after incubation with cGQDs, the number of A549 cells was less than that after incubation with pGQDs, which was consistent with the results of MTT assay, and this further supported the lower cytotoxicity of pGQDs. These results showed that the pGQDs could be used as fluorescent nanoprobes with lower cytotoxicity.

4. CONCLUSIONS

In summary, we presented a simple and green route for enhancing photoluminescence of GQDs by photochemical reduction with isopropanol. After photochemical reduction, the increasing of sp² domains and the formed hydroxyl in pGQDs can enhance the luminescence of GQDs. The pGQDs exhibit strong luminescence with maximum blue emission near 440 nm

and high QY (ca. 8.8%). The obtained pGQDs show lower cytotoxicity and can be more easily uptaken by A549 cells than cGQDs. Our work indicates that photochemical reduction can be used to enhance the QY of GQDs with satisfactory biocompatibility as fluorescent nanoprobe.

■ ASSOCIATED CONTENT

● Supporting Information

Quantum yield of the as-prepared gGQDs, pGQDs and cGQDs. Particle size distributions, height distributions, UV-vis absorption spectra, PL spectra, and upconversion PL spectra at different excitation wavelengths of gGQDs and pGQDs. PL spectra of the CDs and pCDs at different excitation wavelengths. Characterization data (TEM, AFM, FT-IR spectra, XPS analysis, and PL spectra at different excitation wavelengths of cGQDs. Normalized PL spectra of pGQDs converted from gGQDs after different irradiation time and at different light power. This material is available free of charge via the Internet at <http://pubs.acs.org/>.

■ AUTHOR INFORMATION

Corresponding Author

*Fax: (+86) 431-85262656. E-mail: xqu@ciac.jl.cn.

Notes

The authors declare no competing financial interest.

■ ACKNOWLEDGMENTS

This work was supported by the National Basic Research Program of China (2011CB936004, 2012CB720602), and NSFC (21210002, 91213302).

■ REFERENCES

- (1) Sun, X. M.; Liu, Z.; Welsher, K.; Robinson, J. T.; Goodwin, A.; Zaric, S.; Dai, H. J. *Nano Res.* **2008**, *1*, 203–212.
- (2) Shen, J. H.; Zhu, Y. H.; Yang, X. L.; Li, C. Z. *Chem. Commun.* **2012**, *48*, 3686–3699.
- (3) Zhu, S. J.; Tang, S. J.; Zhang, J. H.; Yang, B. *Chem. Commun.* **2012**, *48*, 4527–4539.
- (4) Li, L. L.; Ji, J.; Fei, R.; Wang, C. Z.; Lu, Q.; Zhang, J. R.; Jiang, L. P.; Zhu, J. J. *Adv. Funct. Mater.* **2012**, *22*, 2971–2979.
- (5) Shen, J. H.; Zhu, Y. H.; Chen, C.; Yang, X. L.; Li, C. Z. *Chem. Commun.* **2011**, *47*, 2580–2582.
- (6) Zheng, H. Z.; Wang, Q. L.; Long, Y. J.; Zhang, H. J.; Huang, X. X.; Zhu, R. *Chem. Commun.* **2011**, *47*, 10650–10652.
- (7) Chien, C. T.; Li, S. S.; Lai, W. J.; Yeh, Y. C.; Chen, H. A.; Chen, I. S.; Chen, L. C.; Chen, K. H.; Nemoto, T.; Isoda, S.; Chen, M. W.; Fujita, T.; Eda, G.; Yamaguchi, H.; Chhowalla, M.; Chen, C. W. *Angew. Chem., Int. Ed.* **2012**, *51*, 6662–6666.
- (8) Cote, L. J.; Cruz-Silva, R.; Huang, J. X. *J. Am. Chem. Soc.* **2009**, *131*, 11027–11032.
- (9) Mallik, K.; Mandal, M.; Pradhan, N.; Pal, T. *Nano Lett.* **2001**, *1*, 319–322.
- (10) Sakamoto, M.; Tachikawa, T.; Fujitsuka, M.; Majima, T. *Adv. Funct. Mater.* **2007**, *17*, 857–862.
- (11) Gonzalez, C. M.; Liu, Y.; Scaiano, J. C. *J. Phys. Chem. C* **2009**, *113*, 11861–11867.
- (12) Li, H.; Pang, S.; Feng, X.; Mullen, K.; Bubeck, C. *Chem. Commun.* **2010**, *46*, 6243–6245.
- (13) Zhang, J. L.; Yang, H. J.; Shen, G. X.; Cheng, P.; Zhang, J. Y.; Guo, S. W. *Chem. Commun.* **2010**, *46*, 1112–1114.
- (14) Liu, K. P.; Zhang, J. J.; Cheng, F. F.; Zheng, T. T.; Wang, C. M.; Zhu, J. J. *J. Mater. Chem.* **2011**, *21*, 12034–12040.
- (15) Hummers, W. S.; Offeman, R. E. *J. Am. Chem. Soc.* **1958**, *80*, 1339–1339.

(16) Wang, X. H.; Qu, K. G.; Xu, B. L.; Ren, J. S.; Qu, X. G. *Nano Res.* **2011**, *4*, 908–920.

(17) Shi, P.; Qu, K. G.; Wang, J. S.; Li, M.; Ren, J. S.; Qu, X. G. *Chem. Commun.* **2012**, *48*, 7640–7642.

(18) Li, M.; Yang, X. J.; Ren, J. S.; Qu, K. G.; Qu, X. G. *Adv. Mater.* **2012**, *24*, 1722–1728.

(19) Pan, D. Y.; Guo, L.; Zhang, J. C.; Xi, C.; Xue, Q.; Huang, H.; Li, J. H.; Zhang, Z. W.; Yu, W. J.; Chen, Z. W.; Li, Z.; Wu, M. H. *J. Mater. Chem.* **2012**, *22*, 3314–3318.

(20) Pan, D. Y.; Zhang, J. C.; Li, Z.; Wu, M. H. *Adv. Mater.* **2010**, *22*, 734–738.

(21) Eda, G.; Lin, Y. Y.; Mattevi, C.; Yamaguchi, H.; Chen, H. A.; Chen, I. S.; Chen, C. W.; Chhowalla, M. *Adv. Mater.* **2010**, *22*, 505–509.

(22) Zhu, S. J.; Zhang, J. H.; Qiao, C. Y.; Tang, S. J.; Li, Y. F.; Yuan, W. J.; Li, B.; Tian, L.; Liu, F.; Hu, R.; Gao, H. N.; Wei, H. T.; Zhang, H.; Sun, H. C.; Yang, B. *Chem Commun* **2011**, *47*, 6858–6860.

(23) Dong, Y. Q.; Chen, C. Q.; Zheng, X. T.; Gao, L. L.; Cui, Z. M.; Yang, H. B.; Guo, C. X.; Chi, Y. W.; Li, C. M. *J. Mater. Chem.* **2012**, *22*, 8764–8766.

(24) Asati, A.; Santra, S.; Kaittanis, C.; Perez, J. M. *ACS Nano* **2010**, *4*, 5321–5331.